25th Symposium on Naval Hydrodynamics
St. Johns, Newfoundland and Labrador, CANADA, 8-13 August 2004

Validation of Ship Motion Predictions with Sea Trials Data for a Naval Destroyer in Multidirectional Seas

Kevin McTaggart and Dave Stredulinsky
(Defence R&D Canada - Atlantic, Canada)

ABSTRACT

This paper presents comparisons of ship motion predictions with measured motions for the Canadian naval destroyer HMCS Nipigon in seaways with significant wave heights ranging from 3.7 m to 5.8 m. The numerical predictions include modelling of encountered directional seaways, which were measured by a directional wave buoy. Motions were predicted using a strip theory code and with DRDC Atlantic's new ShipMo3D library, which uses a panel method based on the frequency domain Green function for zero forward speed. To investigate the influence of appendages on radiation forces, frequency domain computations included treatment of the combined panelled hull and panelled appendages. Time domain computations were performed for both linear and nonlinear evaluation of hull forces due to buoyancy and incident waves. Agreement between predicted and observed RMS motions and zero-crossing periods is generally good. Differences between results from the five different sets of predictions are relatively minor.

INTRODUCTION

Predictions of ship motions in waves are being used by navies for a widening number of applications. In the past, ship motion predictions have been used primarily for engineering design applications. In recent years, there has been increasing interest in ship motion predictions by naval operators due to the influence of ship motions on safety and operational effectiveness. Search and rescue missions and ship-borne helicopter operations are examples where ship motions must be duely considered. Ship motions also influence the effectiveness of crew, weapon systems, and sensor systems. The recent trend toward large-scale simulations of military systems is creating increased demand for modelling of ship motions and their influence on ship systems. Depending on simulation requirements, appropriate trade-offs must be made between computational requirements and prediction fidelity.

To address ongoing requirements for ship motion predictions, DRDC Atlantic is developing the ShipMo3D library for simulation of ship motions and sea loads in waves. The library includes modules for computations in both the frequency and time domains. For time domain computations, nonlinear computations of buoyancy and incident wave forces are available. To meet requirements of military simulation applications, it is intended that computations be available that can run faster than real-time without significantly compromising prediction fidelity.

Validation with experimental data is an essential part of development of any ship motion prediction code. When considering the relative merits of model tank tests and full-scale trials, model tank tests typically have the advantages of lower costs, greater control over encountered conditions, and completeness of data. However, full-scale trials are considered essential because they include phenomena that can be absent in model tests due to oversight or scaling effects. Consequently, both full-scale trials and model tests are recommended for validation of numerical ship motion predictions. To support ongoing validation efforts, DRDC typically conducts one or two sea trials per year measuring

ship motions and sea loads in waves. The trials are usually held off the coast of Nova Scotia in the winter months, when rougher sea conditions are more likely to occur. This paper describes the validation of ship motion predictions with sea trial data for the destroyer HMCS Nipigon.

OVERVIEW OF SHIPMO3D LIBRARY FOR PREDICTING SHIP MOTIONS IN WAVES

DRDC Atlantic has been an active developer, user, and sponsor of codes for predicting ship motions and sea loads since the 1970s. Several different codes are currently used, with each code having its own particular strengths and weaknesses. The in-house strip theory code SHIPMO7 (McTaggart et al. 1997, McTaggart 2000) was originally developed by Schmitke (1978) and has a large user base. Other codes for which DRDC Atlantic has been a co-sponsor are used when time domain predictions are required or when three-dimensional hydrodynamic effects are important.

The ShipMo3D library is an effort to consolidate ship motion prediction capabilities into a unified entity that will satisfy a range of application requirements. ShipMo3D uses a panel method to provide enhanced accuracy relative to strip theory, and to ensure applicability to the range of vessels operated by the Canadian Navy. Hydrodynamic coefficients are computed in the frequency domain based on the Green function for zero forward speed, similar to approaches presented by Beck and Loken (1989) and Papanikolaou and Schellin (1992). The decision to use this method was based partly on the relatively slow speeds of present and anticipated Canadian naval vessels, which operate at Froude numbers less than 0.4. Other considerations included computational efficiency and robustness relative to methods using non-zero forward speed Green functions in either the time or frequency domains. Comparisons with experiments presented by McTaggart et al. (1997) and Schellin et al. (2002) indicate that the zero forward speed Green function can lead to very good motion and sea load predictions at moderate ship speeds.

The ShipMo3D library provides motion predictions in both the frequency and time domains. For time domain predictions, hydrodynamic coefficients, including retardation functions, are determined from previously computed frequency domain values, similar to the approach used by Ballard et al. (2003). Comparisons of hydrodynamic forces and motions for the frequency and time domains have verified correct prediction of time domain coefficients from frequency domain coefficients.

Motions are currently computed for a ship travelling at nominally steady speed and heading. Motion computations are performed using a translating earth axis system. Nonlinear buoyancy and incident wave forces can be evaluated based on the instantaneous wetted surface. Nonlinear buoyancy and incident wave forces are initially computed in a ship-fixed axis system and then rotated to the translating earth axis system. Other hydrodynamic forces (i.e., added mass, retardation, and wave diffraction) are assumed to maintain their translating earth axis system values regardless of large amplitude ship motions.

SHIPMO3D APPENDAGE FORCE PREDICTIONS

Sway, roll, and yaw motions are significantly influenced by appendage forces. In addition, viscous forces acting on the ship hull make a noticeable contribution to roll damping. These forces are modelled in ShipMo3D based on approaches presented by Schmitke (1978) and Himeno (1981). Unfortunately, roll motions continue to present a significant challenge for ship motion codes due to difficulties in predicting roll damping components.

When examining methods for predicting viscous roll damping components, there is great variability in predicted values for bilge keel drag forces. The viscous roll moment acting on a bilge keel can be expressed as:

$$F_4^{bk-v} = \frac{1}{2}\,\rho\,\dot{\eta}_4^2 \int_{x_{aft}}^{x_{fore}} C_d(x)\,s(x)\,\widetilde{r}_{BK}^3(x)\,dx \quad (1)$$

where ρ is water density, $\dot{\eta}_4$ is roll velocity, x_{aft} and x_{fore} are the aft and forward longitudinal coordinates of the bilge keel, $C_d(x)$ is the local drag coefficient, and $s(x)$ is the local span. The effective cube of the local viscous roll moment arm, $\widetilde{r_v^3}(x)$, is given by:

$$\widetilde{r}_{BK}^3(x) = r_{BK}^3(x)\;(y\,\cos\Gamma + z\,\sin\Gamma)^2 \quad (2)$$

where $r_{BK}(x)$ is the radius from the local bilge keel center to the ship center of gravity (CG), y is the

lateral coordinate (+ port) relative to the ship CG, Γ is the dihedral angle of the bilge keel relative to horizontal (+ upward), and z is the vertical coordinate (+ upward) relative to the ship CG. Neglecting hull interaction and free surface effects, a long flat plate normal to flow will have a drag coefficient of approximately 1.2. In contrast, bilge keel drag coefficients given by Lloyd (1989) vary between 2 and 12, with the upper value occurring for small amplitude roll motions.

DRDC Atlantic's strip theory code SHIPMO7 models bilge keel viscous drag using the approach described by Schmitke (1978) based on the work of Kato (1966). Kato's formulation is quite complicated, but can be simplified to the following for a representative destroyer:

$$C_d(x) \approx 5 \left(\frac{r_{BK}(x)\, \widehat{\eta}_4\, \omega_e}{\sqrt{g\, s(x)}} \right)^{-0.6} \times \left[1.0 + 3.5 \exp\left(\frac{-11 R_{bilge}(x)}{r_{BK}(x)} \right) \right] \quad (3)$$

where $R_{bilge}(x)$ is the local bilge radius of the hull, $\widehat{\eta}_4$ is roll amplitude, and ω_e is wave encounter frequency. Perhaps the most noteworthy feature of Equation (3) is the large degree of variation of the drag coefficient with roll velocity amplitude $\widehat{\eta}_4\, \omega_e$. When considering Equations (1) and (3) together, the proportionality of viscous roll drag to $(\widehat{\eta}_4\, \omega_e)^{1.4}$ combined with the presence of gravitational acceleration in Equation (3) possibly arise from trying to model radiation and viscous forces simultaneously.

The ShipMo3D library currently models the bilge keel drag coefficients as follows:

$$C_d = C_{d-ref}(\widehat{\eta}_{4-ref}) \left(\frac{\widehat{\dot{\eta}}_4}{\widehat{\dot{\eta}}_{4-ref}} \right)^{-\alpha} \quad (4)$$

where C_{d-ref} is an input reference drag coefficient for roll velocity amplitude $\widehat{\dot{\eta}}_{4-ref}$ and α is an input decay exponent. This approach provides flexibility in the selection of bilge keel roll damping coefficients, including the possibilities of using input values from experiments or CFD computations.

Appendage force predictions by Schmitke neglect free-surface effects. The influence of the hull on appendage potential flow forces is modelled by assuming that the local hull is a planar boundary. The influence of the appendages on hull forces is neglected. The ShipMo3D library introduces an option for including appendages in hull radiation and diffraction computations by assuming that appendages are thin and modelling them using dipole panels (Chakrabarti, 1987). Due to the significant variation of dipole strengths across a flat plate (Meyerhoff, 1970), each appendage typically has several panels in each of the span-wise and chord-wise directions.

NAVAL DESTROYER HMCS NIPIGON

The naval destroyer HMCS Nipigon (Figure 1) was the subject of a comprehensive sea trial measuring ship motions and sea loads in December 1997. HMCS Nipigon was the last steam-driven destroyer in the Canadian Fleet. Figure 2 gives a body plan for Nipigon and Table 1 gives particulars. Nipigon appendages include 2 rudders, 2 outer propeller shaft brackets, 2 inner propeller shaft brackets, 2 bilge keels, and a skeg, with dimensions as given in Table 2.

Figure 1: HMCS NIPIGON

SEA TRIAL ON HMCS NIPIGON

During the December 1997 sea trial, a series of 71 trial runs of 20 to 30 minute duration was undertaken at two nominal ship speeds in head, bow, beam, quartering and following seas. Data were collected in higher sea states (4, 5 and 6) for three days over December 2, 3 and 4th and for four days at lower sea states (2 and 3) over December 8 to 11th. The 'low' ship speed was about 8 knots and

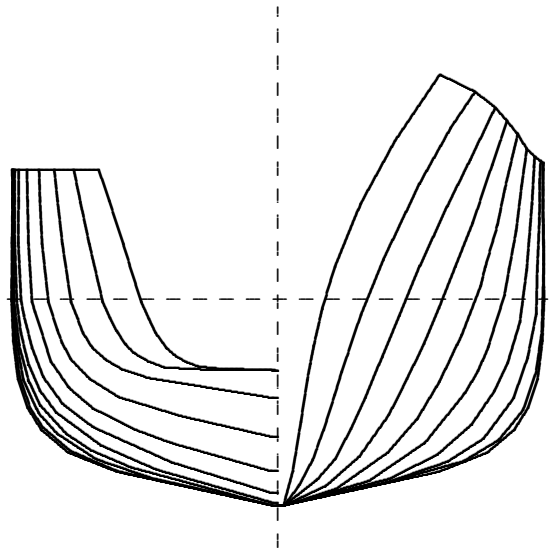

Figure 2: Body Plan for HMCS Nipigon

Table 1: Particulars for HMCS Nipigon

Displacement	3027 tonnes
Length between perpendiculars	108.4 m
Beam	12.8 m
Draft	4.3 m
Trim by stern	0.5 m
Height of CG above keel	5.1 m
CG from forward perpendicular	57.5 m
Block coefficient	0.503
Prismatic coefficient	0.625
Wetted hull area	1446 m^2
Metacentric height	1.2 m
Roll radius of gyration	5.6 m
Pitch radius of gyration	27.1 m
Natural roll period	10.6 s

Table 2: Appendages for HMCS Nipigon

Rudders (2)	
Station	19.3
Root lateral offset	1.981 m
Root above baseline	3.197 m
Span	3.023 m
Root chord	2.286 m
Tip chord	1.886 m
Dihedral angle (port)	-90 deg
Area (port+starboard)	12.6 m^2
Outer shaft brackets (2)	
Station	18.3
Root lateral offset	3.109 m
Root above baseline	3.200 m
Span	2.256 m
Root chord	0.800 m
Tip chord	0.800 m
Dihedral angle (port)	-99.5 deg
Area (port+starboard)	3.6 m^2
Inner shaft brackets (2)	
Station	18.3
Root lateral offset	1.158 m
Root above baseline	2.957 m
Span	2.240 m
Root chord	0.800 m
Tip chord	0.800 m
Dihedral angle (port)	-64.2 deg
Area (port+starboard)	3.6 m^2
Bilge Keels (2)	
Fore station	8.82
Aft station	13.79
Span	0.610 m
Area (port+starboard)	32.9 m^2
Skeg at Centerline	
Fore station	14.0
Aft station	16.5
Aft span	1.236 m
Area	6.8 m^2

Station 20 is aft perpendicular

'high' ship speed was between 14 and 18 knots depending on what speed the ship could maintain in the given sea state. Speed was limited due to the loss of one of the two ship boilers on the first day of the trial.

Trial instrumentation included a ship motions package, a wave buoy, a TSK over-the-bow wave height meter, an array of 24 pressure transducers outfitted in the hull below the waterline, 15 single strain gauges, and 4 rosette strain gauges. Wave data were collected for 20 minutes out of every hour from the wave buoy. An Endeco type 1156 directional wave buoy was used for the first 3 days of the trial, and a type 956 buoy was used for the last 4 days. Figure 3 shows an Endeco wave buoy being deployed from Nipigon. The main data acquisition system was a PC-based LabVIEW system. All sixty instrumentation channels were digitally sampled at 20 Hz. Time histories, statistical distributions and minimum and maximum values were determined and recorded.

For the present study only the ship motion and wave data have been used. A limited number of runs from the first three days of the trial was selected to satisfy the following 3 criteria:

- the significant wave height H_s was greater than 3 m,
- there was a clear dominant wave direction and minimal directional wave spreading,
- the nominal relative wave direction was oblique (bow quartering, beam, or stern quartering seas).

Table 3 gives a summary of the runs selected for the present study, with T_z denoting zero-crossing wave period. Figure 4 shows an example measured wave spectrum.

Rudder deflections were not measured during the sea trial, and are assumed to have had no effect on ship roll motions. In reality, the rudder motions could have significantly influenced the ship roll motions, particularly if rudder motions were at a frequency similar to the ship natural roll frequency.

Figure 3: Endeco Wave Buoy Being Deployed from HMCS Nipigon

Table 3: NIPIGON Trial Runs Used in Present Study

Run	Speed (kt)	H_s (m)	T_z (s)	Wave dir. (from, deg) Mean	Dev.	Ship head. (to, deg)	Rel. wave head.
203	8	3.73	7.73	218	39	265	BQ
204	8	3.67	7.21	225	39	85	SQ
206	16	3.89	7.39	228	25	355	SQ
209	13	4.75	8.07	224	33	265	BQ
210	15	4.75	8.07	224	33	85	SQ
303	8	5.82	9.45	274	41	310	BQ
304	8	5.57	8.81	272	39	120	SQ
305	8	5.57	8.81	272	39	220	BQ
306	8	5.16	8.66	266	45	50	SQ
309	14	5.39	8.95	279	32	315	BQ
310	14	5.44	8.73	269	43	135	SQ
403	8	5.01	9.34	244	40	290	BQ
404	8	4.90	9.60	238	47	110	SQ
409	16	4.52	8.37	238	50	285	BQ
410	16	4.52	8.37	238	50	105	SQ
413	8	4.98	8.86	245	40	330	Bm

Relative wave headings
BQ - Bow quartering
SQ - Stern quartering
Bm - Beam

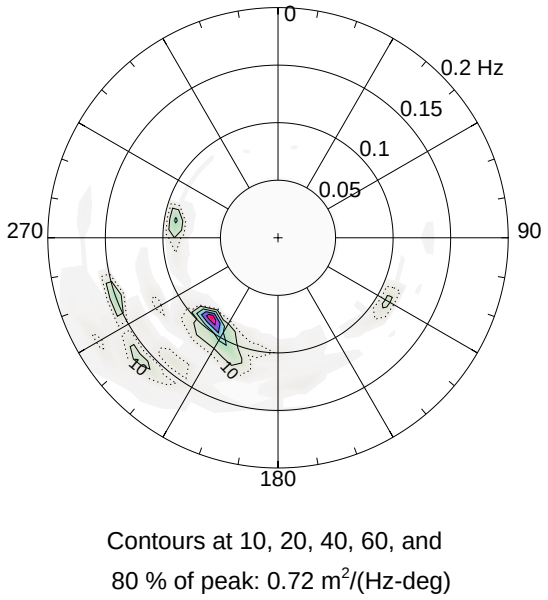

Figure 4: Measured Directional Wave Spectrum for Run 203

NUMERICAL PREDICTIONS OF SEA TRIAL MOTIONS

Numerical predictions of ship motions during sea trial runs were made using the strip theory program SHIPMO7 and with the ShipMo3D library.

All predictions considered the ship motions in the measured short-crested seaways. Four different types of predictions were made using the ShipMo3D library:

- frequency domain predictions, appendages not included in hull radiation and diffraction computations,
- frequency domain predictions, both hull and appendages included in radiation and diffraction computations,
- time domain predictions with linear buoyancy and incident wave forces,
- time domain predictions with nonlinear buoyancy and incident wave forces.

The time domain predictions do not include the appendages in the hull radiation and diffraction computations.

For three-dimensional radiation and diffraction computations, the wet hull was represented by 814 flat panels (407 panels on the port side), with most panels being quadrilaterals and the remainder being triangles. The dry hull, required for computing nonlinear buoyancy and incident wave forces, was represented by a total of 1,276 panels. Figure 5 shows the panelled hull, with the wet portion represented by white panels and the dry portion represented by grey panels. For radiation and diffraction computations including panelling of the appendages, the port and starboard appendages were modelled using 308 panels (154 panels on the port side), and the centerline skeg was modelled using 18 panels. Figure 6 shows the port half of the hull in red, and appendages on the port side and centerline in yellow. Figure 7 shows expanded views of the panelled aft appendages.

Hydrodynamic coefficients in the frequency domain were computed at the zero and infinite frequency limits and at intermediate encounter frequencies of 0.1, 0.2, ..., 6.0 rad/s. For each encounter frequency, computed terms include the zero

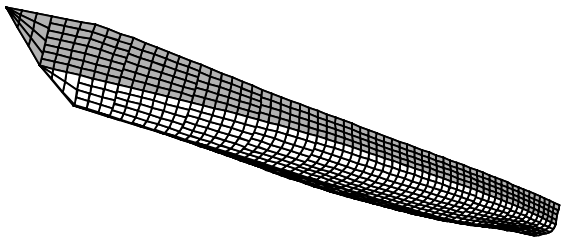

Figure 5: Nipigon Wet (White) and Dry (Grey) Panelled Hull

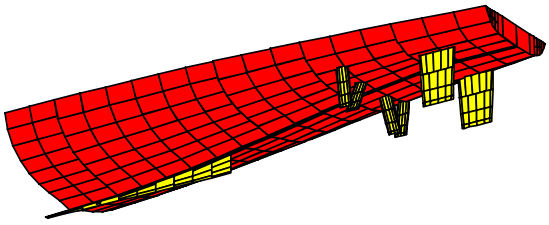

Figure 6: Aft Portion of Nipigon Wet Panelled Hull (Red) with Appendages (Yellow)

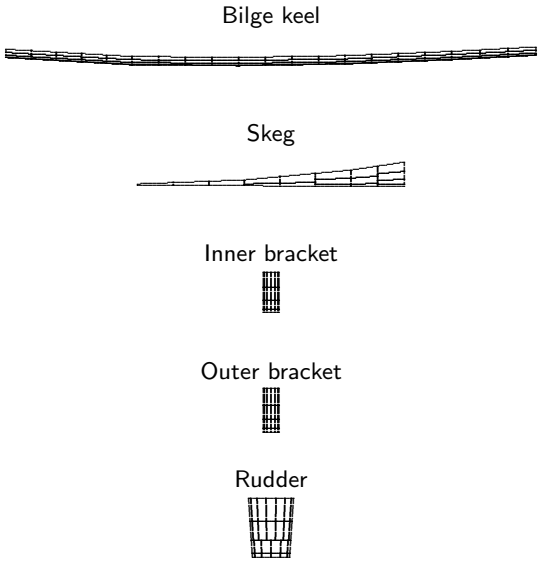

Figure 7: Profiles of Nipigon Panelled Appendages

speed coefficients and terms proportional to ship speed U and U^2 that can be used to evaluate hydrodynamic coefficients at arbitrary forward speed. Wave diffraction terms were evaluated for speeds of 0, 5, ..., 30 knots, relative wave directions of 0, 10, ..., 180 degrees, and wave frequencies of 0.2, 0.3, ..., 2.0 rad/s. The computed hydrodynamic coefficients and diffraction forces form a database from which hydrodynamic forces can be obtained for any seaway encountered by the ship.

For time domain simulations, retardation functions were computed using convolution integrals applied to previously computed frequency domain coefficients. The retardation functions were computed for delay times of 0.0, 0.1, ..., 20 s. Retardation forces are negligible beyond delay times of 20 s. Time domain simulations were conducted using both linear and nonlinear forces from buoyancy and incident waves. For nonlinear incident wave forces, Wheeler stretching (Wheeler, 1970) was used to model the variation of velocity potential with distance below the instantaneous free surface. The time domain simulations used a time step size of 0.2 s and total duration of 30 minutes.

The bilge keel roll damping was modelled using Equation (4) with a reference drag coefficient of 16.5 for the ship rolling with an amplitude of 5 degrees at its natural roll period of 10.6 s. The decay coefficient α has a value of 0.60. Both the reference drag coefficient and decay coefficient were obtained from calculations using Kato's method. Figure 8 shows the variation of bilge keel drag coefficient with roll amplitude for oscillations at the ship natural roll frequency. During time domain computations, it was necessary to select a nominal roll velocity amplitude for computing the bilge keel drag coefficient. At each time step, the nominal roll velocity amplitude was set to 1.25 times the RMS roll velocity during the most recent 20 s of motion. All other appendages were assumed to have constant drag coefficient values of 1.17.

Time domain simulations with the ShipMo3D library currently are limited to a ship with nominally steady speed and heading. Due to the absence of rudder motion data during the sea trial, rudder motions were assumed to be small. This assumption will have little influence on predicted roll motions if the rudder motions were limited to low frequency. To ensure course-keeping, additional stiffness and damping terms given in Table 4 were used for surge, sway, and yaw. The stiffness and

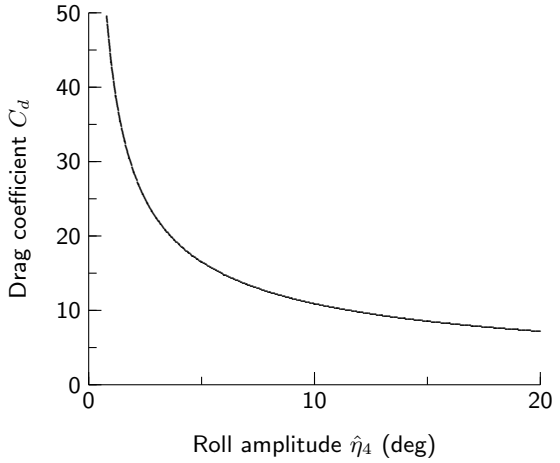

Figure 8: Bilge Keel Drag Coefficient Versus Roll Amplitude at Ship Natural Roll Period of 10.6 s

damping values were selected such that they would have only a minor influence on predicted motions, and are based on natural periods of approximately 100 s and damping of approximately half of critical damping.

Table 4: Additional Stiffness and Damping for Ensuring Course-Keeping with ShipMo3D Computations

	Stiffness	Damping
Surge	1×10^4 N/m	2×10^5 N/(m/s)
Sway	2×10^4 N/m	4×10^5 N/(m/s)
Yaw	2×10^8 Nm/rad	2×10^8 Nm/(rad/s)

Due to strong roll resonance behavior, it is essential that sufficiently fine increments be used for wave frequency and wave direction. The computations in both the frequency and time domains used incident seaway components with wave frequencies of 0.2, 0.25, ..., 2.0 rad/s and absolute wave directions of 0, 10, ..., 360 degrees. For measured directional sea spectra, the number of non-zero wave spectral components within the specified combinations of wave frequency and wave direction ranged from 158 to 323.

For the time domain computations using linear buoyancy and incident wave forces, computational times were approximately three times faster than real-time on an 800 MHz Pentium III desktop computer. When nonlinear buoyancy and incident wave forces were evaluated at each time step on the instantaneous wetted hull, computational times were approximately one third as fast as real-time.

COMPARISONS OF SEA TRIAL DATA AND PREDICTIONS

Tables 5 to 10 give observed and predicted values of RMS displacements and zero-crossing periods for heave, roll, and pitch. Agreement between observed and predicted values is generally good, with the best agreement occurring for heave, followed by pitch and roll, respectively. The five different prediction methods give quite similar results. Figures 9 to 14 show scatter plots of predicted versus observed RMS motions and zero-crossing periods, where the predictions are from time domain simulations with nonlinear buoyancy and Froude-Krylov forces.

INFLUENCE OF APPENDAGE FORCE PREDICTIONS ON ROLL HYDRODYNAMICS

The frequency domain predictions presented in Tables 5 to 10 indicate that including the panelled appendages in radiation and diffraction computations has very little influence on predicted hydrodynamic forces for Nipigon. Figures 15 and 16 show roll added mass and damping versus ship speed for motions at Nipigon's natural roll period of 10.6 s. Added mass is non-dimensionalized by ship roll inertia I_{44}, and damping is non-dimensionalized by critical roll damping at zero speed B_{44}^{cr}. Results are given for zero amplitude roll motions (i.e., viscous roll forces are negligible). Figure 15 indicates that treating the appendages separately from the hull gives slightly higher added mass than when using panelled appendages integrated with the hull radiation computations. As expected, the bare hull has lower added mass than the appended hull. Figure 16 shows that including the panelled appendages in the radiation computations has negligible effect on predicted roll damping, with the relevant plotted lines being indistinguishable.

Table 5: Observed and Predicted RMS Heave (m)

Run	Trial	Strip theory	3D freq. Appendages Sep.	3D freq. Appendages Integ.	3D time Hull forces Linear	3D time Hull forces Nonlin.
203	0.70	0.65	0.66	0.66	0.68	0.68
204	0.55	0.48	0.47	0.47	0.46	0.46
206	0.76	0.60	0.58	0.58	0.59	0.59
209	0.84	0.90	0.96	0.96	0.99	1.00
210	0.89	0.71	0.67	0.67	0.68	0.68
303	1.38	1.10	1.11	1.11	1.01	1.00
304	1.02	0.93	0.90	0.90	0.80	0.80
305	0.98	1.19	1.19	1.19	1.17	1.17
306	0.81	0.97	0.95	0.95	1.00	1.00
309	1.33	1.07	1.12	1.11	1.12	1.13
310	0.97	0.92	0.89	0.89	0.88	0.88
403	1.15	1.00	1.01	1.00	1.05	1.05
404	0.88	0.93	0.92	0.92	0.89	0.89
409	1.13	0.88	0.94	0.94	0.96	0.97
410	0.78	0.74	0.72	0.72	0.72	0.72
413	1.09	1.14	1.15	1.15	1.13	1.13
Predicted/observed						
Mean		0.94	0.94	0.94	0.93	0.94
Deviation		0.14	0.14	0.14	0.15	0.16

Table 6: Observed and Predicted Heave Zero-Crossing Period (s)

Run	Trial	Strip theory	3D freq. Appendages Sep.	3D freq. Appendages Integ.	3D time Hull forces Linear	3D time Hull forces Nonlin.
203	8.1	8.4	8.2	8.3	8.2	8.2
204	9.3	10.3	10.2	10.2	10.3	10.2
206	11.8	10.5	10.2	10.2	10.1	10.1
209	7.3	7.0	6.8	6.9	6.8	6.8
210	11.7	12.0	11.7	11.7	11.5	11.5
303	9.7	9.8	9.7	9.7	9.7	9.6
304	12.2	13.3	13.3	13.3	12.9	12.7
305	8.6	8.7	8.5	8.5	8.3	8.3
306	11.1	10.8	10.6	10.7	10.6	10.6
309	9.6	8.2	7.9	7.9	7.8	7.8
310	11.7	13.3	13.1	13.1	13.3	13.2
403	10.0	9.5	9.3	9.4	9.4	9.5
404	11.2	12.3	12.3	12.3	12.1	12.1
409	8.3	7.5	7.2	7.2	7.0	7.0
410	11.3	12.2	11.8	11.8	11.5	11.5
413	10.2	8.8	8.7	8.7	8.7	8.7
Predicted/observed						
Mean		1.00	0.98	0.98	0.97	0.97
Deviation		0.09	0.09	0.09	0.09	0.09

Table 7: Observed and Predicted RMS Roll (deg)

Run	Trial	Strip theory	3D freq. Appendages Sep.	3D freq. Appendages Integ.	3D time Hull forces Linear	3D time Hull forces Nonlin.
203	2.83	3.37	4.03	4.12	3.67	3.73
204	3.97	4.28	4.76	4.80	4.22	4.27
206	4.25	5.15	5.93	6.09	5.47	5.59
209	2.64	2.54	3.11	3.23	3.02	3.21
210	4.98	4.97	5.85	6.00	5.99	6.19
303	4.95	5.24	5.40	5.49	4.90	4.89
304	6.16	4.91	5.30	5.36	4.66	4.73
305	3.18	5.35	5.58	5.67	4.75	4.89
306	4.46	6.17	6.32	6.40	5.88	5.93
309	3.93	3.45	4.12	4.28	3.75	4.06
310	5.41	3.91	4.92	5.02	4.64	4.78
403	3.95	4.60	5.09	5.17	4.68	4.75
404	4.26	4.75	5.19	5.26	4.49	4.56
409	2.63	2.68	3.58	3.72	3.47	3.70
410	3.75	3.46	4.11	4.22	4.42	4.56
413	4.24	6.15	6.24	6.33	5.72	5.77
Predicted/observed						
Mean		1.10	1.24	1.27	1.15	1.19
Deviation		0.24	0.22	0.22	0.19	0.20

Table 8: Observed and Predicted Roll Zero-Crossing Period (s)

Run	Trial	Strip theory	3D freq. Appendages Sep.	3D freq. Appendages Integ.	3D time Hull forces Linear	3D time Hull forces Nonlin.
203	9.2	9.7	9.8	9.7	9.8	9.9
204	10.2	10.5	10.5	10.5	10.3	10.5
206	12.3	11.0	11.0	11.0	10.8	10.9
209	8.4	8.5	8.8	8.7	8.8	8.9
210	12.3	11.8	11.7	11.7	11.5	11.5
303	9.5	10.6	10.5	10.5	10.7	10.5
304	11.0	10.9	10.8	10.8	10.7	10.7
305	8.8	10.0	10.0	9.9	10.0	9.9
306	10.7	10.4	10.4	10.4	10.2	10.3
309	9.1	9.6	9.8	9.7	9.7	9.5
310	11.5	12.1	11.8	11.8	12.4	12.4
403	10.0	10.3	10.3	10.3	10.2	10.3
404	10.7	10.7	10.7	10.7	10.5	10.4
409	9.5	9.7	10.1	10.0	9.8	9.8
410	12.1	12.6	12.4	12.3	11.8	12.0
413	10.0	10.2	10.1	10.1	9.9	9.8
Predicted/observed						
Mean		1.02	1.02	1.02	1.02	1.02
Deviation		0.06	0.06	0.05	0.06	0.06

Table 9: Observed and Predicted RMS Pitch (deg)

Run	Trial	Strip theory	3D freq. Appendages		3D time Hull forces	
			Sep.	Integ.	Linear	Nonlin.
203	1.03	1.14	1.18	1.18	1.19	1.21
204	0.79	0.93	0.88	0.88	0.89	0.90
206	1.00	1.01	0.88	0.88	0.93	0.94
209	1.45	1.83	1.96	1.96	2.02	2.04
210	1.08	1.23	1.10	1.10	1.19	1.21
303	1.66	1.98	2.05	2.05	1.80	1.84
304	1.51	1.39	1.29	1.29	1.26	1.28
305	1.89	1.72	1.79	1.79	1.83	1.85
306	1.44	1.34	1.29	1.29	1.32	1.34
309	1.59	1.84	1.98	1.98	1.99	2.00
310	1.21	1.31	1.22	1.22	1.24	1.25
403	1.37	1.64	1.71	1.71	1.83	1.86
404	1.08	1.29	1.24	1.24	1.31	1.33
409	1.59	1.62	1.75	1.74	1.74	1.75
410	1.04	1.13	1.07	1.07	1.11	1.13
413	1.10	1.21	1.26	1.26	1.25	1.28
Predicted/observed						
Mean		1.09	1.09	1.09	1.10	1.12
Deviation		0.10	0.14	0.14	0.15	0.15

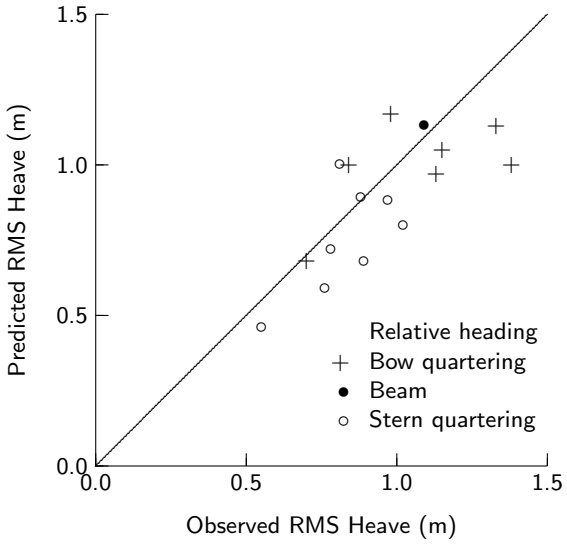

Figure 9: Predicted Versus Observed RMS Heave, Time Domain Predictions with Nonlinear Buoyancy and Incident Wave Forces

Table 10: Observed and Predicted Pitch Zero-Crossing Period (s)

Run	Trial	Strip theory	3D freq. Appendages		3D time Hull forces	
			Sep.	Integ.	Linear	Nonlin.
203	6.3	7.3	7.2	7.2	7.1	7.1
204	7.9	10.0	9.8	9.8	10.1	10.1
206	12.1	11.6	11.4	11.4	11.1	11.0
209	5.8	6.2	6.2	6.2	6.2	6.2
210	10.1	13.6	13.4	13.4	14.5	14.6
303	7.3	7.8	7.8	7.8	7.5	7.5
304	10.8	12.5	12.6	12.6	12.8	12.8
305	7.3	7.0	6.9	6.9	6.9	6.8
306	11.4	10.8	10.4	10.4	10.3	10.5
309	6.7	6.3	6.3	6.3	6.1	6.2
310	10.3	14.1	13.7	13.7	13.9	13.9
403	7.7	7.5	7.5	7.5	7.9	7.9
404	9.2	11.6	11.4	11.4	11.6	11.7
409	6.5	6.0	5.9	5.9	5.9	5.9
410	10.2	12.6	11.9	11.9	12.2	12.2
413	8.0	7.3	7.1	7.1	7.1	7.1
Predicted/observed						
Mean		1.10	1.08	1.08	1.09	1.09
Deviation		0.16	0.15	0.15	0.17	0.17

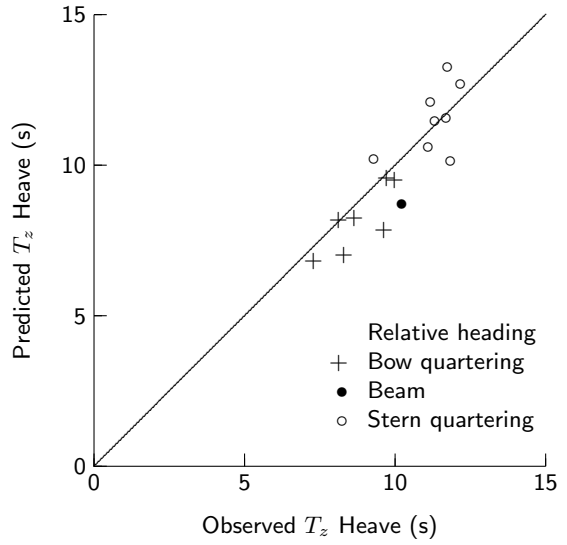

Figure 10: Predicted Versus Observed Heave Zero-Crossing Period, Time Domain Predictions with Nonlinear Buoyancy and Incident Wave Forces

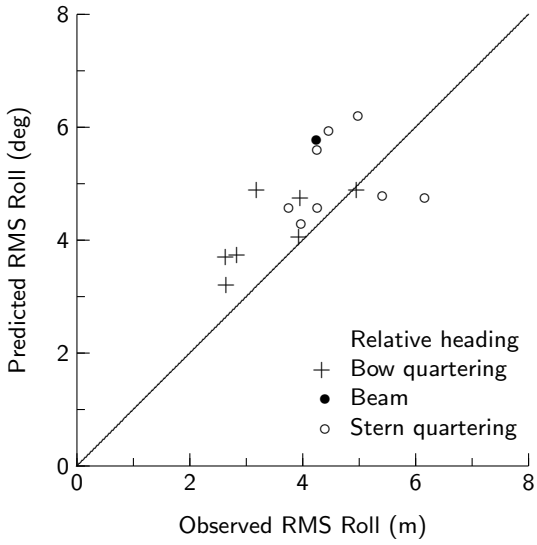

Figure 11: Predicted Versus Observed RMS Roll, Time Domain Predictions with Nonlinear Buoyancy and Incident Wave Forces

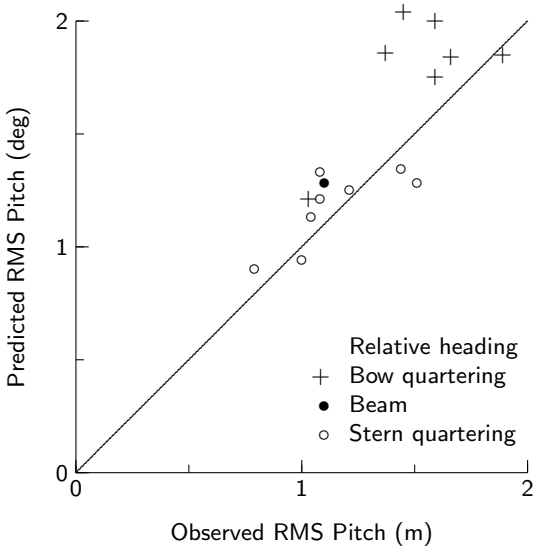

Figure 13: Predicted Versus Observed RMS Pitch, Time Domain Predictions with Nonlinear Buoyancy and Incident Wave Forces

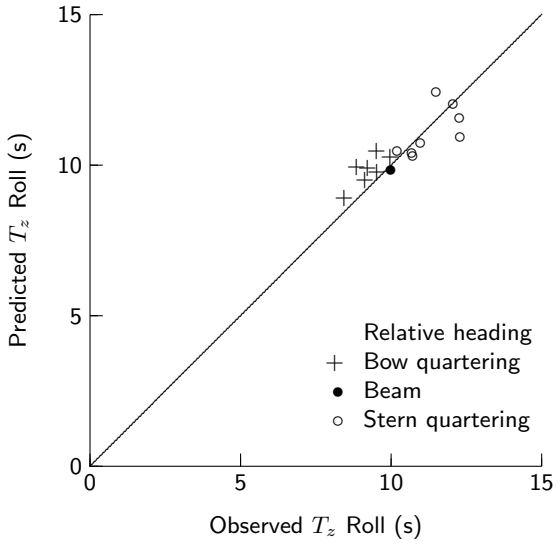

Figure 12: Predicted Versus Observed Roll Zero-Crossing Period, Time Domain Predictions with Nonlinear Buoyancy and Incident Wave Forces

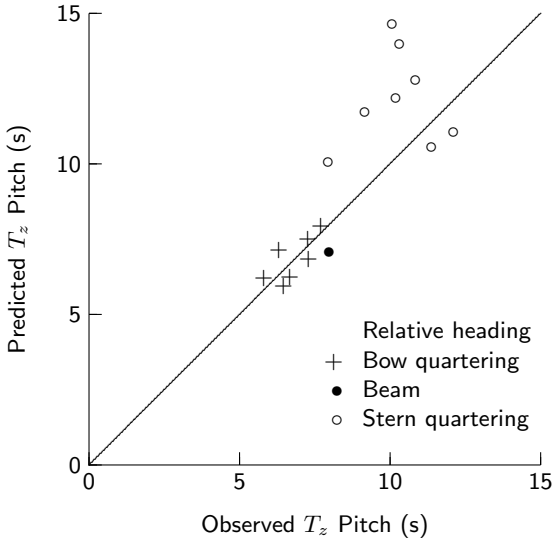

Figure 14: Predicted Versus Observed Pitch Zero-Crossing Period, Time Domain Predictions with Nonlinear Buoyancy and Incident Wave Forces

DISCUSSION

The Nipigon sea trial included simultaneous measurements of ship motions and directional wave spectra. Measurements of rudder motions would have enhanced the value of the data for validation of lateral plane motion predictions. In the absence of measured rudder motions, coursekeeping has been modelled using low frequency stiffness terms, and associated damping terms, for surge, sway and yaw.

The numerical predictions give generally good agreement with the RMS motions and zero-crossing periods during the Nipigon sea trial. As expected, agreement is better for heave and pitch than for roll. Among the numerical prediction methods, the predicted motions are very similar. The good results from strip theory are likely due to Nipigon's slender geometry. Time domain predictions using linear and nonlinear forces from buoyancy and incident waves give very similar results, likely due to Nipigon having minimal flare near the waterline at most stations.

The negligible influence of panelled appendages on the roll radiation damping is likely due to the small appendage sizes relative to the hull and to the degree of submergence of the appendages. Larger appendages located closer to the free surface would have a larger influence on roll radiation damping. For Nipigon and other ships with small appendages of large submergence, it appears unnecessary to include panelled appendages in radiation and diffraction computations.

The scattergrams in Figures 9 to 14 provide further insight into trends. The overprediction of RMS roll appears to be similar for bow quartering and stern quartering seas. The underprediction of viscous appendage forces is a possible cause for overprediction of RMS roll. For RMS pitch, there is a trend toward overprediction in bow quartering seas, which could be due to higher amplitude motions. Pitch zero-crossing periods exhibit a trend toward overprediction in stern quartering seas, possibly due to the assumption of high encounter frequency when considering forward speed effects.

Accurate prediction of viscous roll damping forces is still considered to be a major challenge for obtaining accurate ship motion predictions. The current motion predictions using Kato's method (1966) for bilge keel roll damping give reasonable roll results. However, the roll motions presented

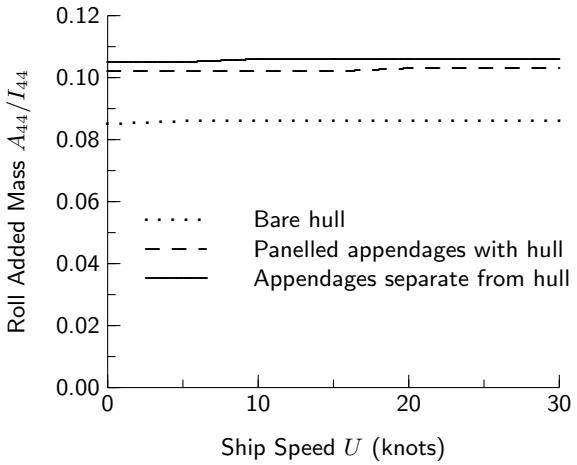

Figure 15: Nipigon Roll Added Mass Versus Ship Speed at Roll Natural Period of 10.6 s, Zero Roll Amplitude

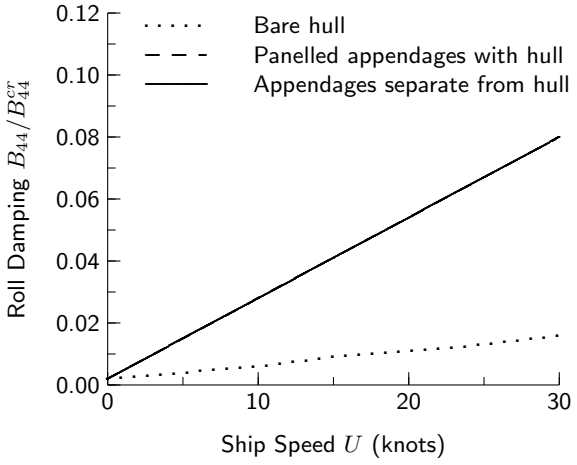

Figure 16: Nipigon Roll Damping Versus Ship Speed at Roll Natural Period of 10.6 s, Zero Roll Amplitude

from the Nipigon trial are limited to relatively narrow ranges of RMS values (2.63 to 6.16 degrees) and zero-crossing periods (8.4 to 13.2 s). It is essential that roll motions be validated over wide ranges of motion amplitudes and frequencies.

CONCLUSIONS

Numerical predictions have been compared with measured heave, roll, and pitch for a naval destroyer in multidirectional seas. The numerical predictions give generally good agreement with measured RMS motions and zero-crossing periods. Strip theory and three-dimensional predictions give very similar results, likely because of the slender hull form of the destroyer HMCS Nipigon. The influence of appendage radiation forces has been investigated by including panelled appendages in radiation computations. For Nipigon, inclusion of appendages in radiation computations has negligible effect on predicted motions in comparison with the commonly used approach of treating appendages separately from the hull and assuming deep submergence. Evaluation of nonlinear buoyancy and incident wave forces based on the instantaneous wetted hull surface has only a minor influence on predicted motions relative to those assuming linear hull forces.

REFERENCES

Ballard, E.J., Hudson, D.A., Price, W.G. and Temarel, P., "Time Domain Simulation of Symmetric Ship Motions in Waves", *International Journal of Maritime Engineering*, Vol. 143, No. A3, 2003, pp. 1–20.

Beck, R.F. and Loken, A.E., "Three–Dimensional Effects in Ship Relative–Motion Problems", *Journal of Ship Research*, Vol. 33, 1989, pp. 261–268.

Chakrabarti, S.K., *Hydrodynamics of Offshore Structures*, Springer-Verlag, 1987.

Himeno, Y., "Prediction of Ship Roll Damping - State of the Art", Report 239, 1981, Department of Naval Architecture and Marine Engineering, University of Michigan.

Kato, H., "Effects of Bilge Keels on the Roll Damping of Ships", *Memories of the Defence Academy, Japan*, Vol. 4, 1966.

Lloyd, A.R.J.M., *Seakeeping: Ship Behaviour in Rough Weather*, Ellis Horwood, Chichester, England, 1989.

McTaggart, K., "Lateral Ship Motions and Sea Loads in Waves Including Appendage and Viscous Forces", *International Shipbuilding Progress*, Vol. 47, 2001, pp. 141–160.

McTaggart, K., Datta, I., Stirling, A., Gibson, S., and Glen, I., "Motions and Loads of a Hydroelastic Frigate Model in Severe Seas", *Transactions, Society of Naval Architects and Marine Engineers*, Vol. 105, 1997.

Meyerhoff, W.K., "Added Mass of Thin Rectangular Plates Calculated from Potential Theory", *Journal of Ship Research*, Vol. 4, 1970, pp. 100–111.

Papanikolaou, A.D. and Schellin, T.E., "A Three–Dimensional Panel Method for Motions and Loads of Ships with Forward Speed", *Schiffstechnik (Ship Technology Research)*, Vol. 39, 1992, pp. 147–156.

Schellin, T.E., Chen, X.-B., Beiersdorf, C. and Maron, A., "Comparative Frequency Domain Seakeeping Analysis of a Fast Monohull in Regular Head Waves", *21st International Conference on Offshore Mechanics and Arctic Engineering*, Oslo, 2002.

Schmitke, R.T., "Ship Sway, Roll, and Yaw Motions in Oblique Seas", *Transactions, Society of Naval Architects and Marine Engineers*, Vol. 86, 1978, pp. 26–46.

Wheeler, D.J, "Method for Prediction of Forces Produced by Irregular Waves", *Journal of Petroleum Technology*, 1970, pp. 359–367.